AGU PUBLICATIONS

JGR

Journal of Geophysical Research: Biogeosciences

RESEARCH ARTICLE
10.1002/2017JG004232

Key Points:
- UAVs can map peatland CH_4 controlling factors (surface morphology and hydrology) over large areas
- From these data we derive the first estimate of seismic line impacts on CH_4 emission in a forested bog

Supporting Information:
- Supporting Information S1

Correspondence to:
J. Lovitt,
julie.lovitt@ucalgary.ca

Citation:
Lovitt, J., Rahman, M. M., Saraswati, S., McDermid, G. J., Strack, M., & Xu, B. (2018). UAV remote sensing can reveal the effects of low-impact seismic lines on surface morphology, hydrology, and methane (CH_4) release in a boreal treed bog. *Journal of Geophysical Research: Biogeosciences*, *123*. https://doi.org/10.1002/2017JG004232

Received 18 OCT 2017
Accepted 18 FEB 2018
Accepted article online 23 FEB 2018

UAV Remote Sensing Can Reveal the Effects of Low-Impact Seismic Lines on Surface Morphology, Hydrology, and Methane (CH_4) Release in a Boreal Treed Bog

J. Lovitt[1], M. M. Rahman[1], S. Saraswati[2], G. J. McDermid[1], M. Strack[2], and B. Xu[3]

[1]Department of Geography, University of Calgary, Calgary, Alberta, Canada, [2]Department of Geography, University of Waterloo, Waterloo, Ontario, Canada, [3]Northern Alberta Institute of Technology, Edmonton, Alberta, Canada

Abstract Peatlands are globally significant stores of soil carbon, where local methane (CH_4) emissions are strongly linked to water table position and microtopography. Historically, these factors have been difficult to measure in the field, constraining our capacity to observe local patterns of variability. In this paper, we show how remote sensing surveys conducted from unmanned aerial vehicle (UAV) platforms can be used to map microtopography and depth to water over large areas with good accuracy, paving the way for spatially explicit estimates of CH_4 emissions. This approach enabled us to observe—for the first time—the effects of low-impact seismic lines (LIS; petroleum exploration corridors) on surface morphology and CH_4 emissions in a treed-bog ecosystem in northern Alberta, Canada. Through compaction, LIS lines were found to flatten the observed range in microtopographic elevation by 46 cm and decrease mean depth to water by 15.4 cm, compared to surrounding undisturbed conditions. These alterations are projected to increase CH_4 emissions by 20–120% relative to undisturbed areas in our study area, which translates to a total rise of 0.011–0.027 kg CH_4 day^{-1} per linear kilometer of LIS (~2 m wide). The ~16 km of LIS present at our 61 ha study site were predicted to boost CH_4 emissions by 20–70 kg between May and September 2016.

1. Introduction

Peatlands—wetlands that accumulate organic matter—can release large volumes of carbon into the atmosphere in response to anthropogenic disturbances (Wieder & Vitt, 2006; Strack et al., 2006; Parish et al., 2008; Vitt & Bhatti, 2012; Munir et al., 2014). Of particular concern is CH_4: a powerful greenhouse gas (GHG) with a 20 year global warming potential 84 times greater than that of carbon dioxide (Intergovernmental Panel on Climate Change (IPCC), 2014a; Zhu et al., 2014). The Intergovernmental Panel on Climate Change states that CH_4 emissions from wetlands are the primary driver of variability in atmospheric CH_4 concentrations (IPCC, 2013). However, the processes relating anthropogenic disturbance to wetland CH_4 production and emission rates are both highly variable and poorly quantified, ultimately limiting our capacity to generate reliable global CH_4 estimates (IPCC, 2014b).

CH_4 flux is difficult to observe directly, and most nonpoint estimates rely on modeled associations with environmental covariates (Xu et al., 2010). For example, previous research has shown that CH_4 is released in greater volumes in peatlands when water table (WT) is at or near the surface (Wieder & Vitt, 2006), and numerous studies have observed that much of the variability in peatland CH_4 flux can be explained by differences in WT position (Couwenberg & Fritz, 2012; Kellner et al., 2005). WT estimates are commonly derived through repeated field measurements using monitoring wells (Lee & Cherry, 1979; Vazquez-Amábile & Engel, 2005). However, this method is time-consuming and spatially limited to single observation points.

As an alternative or complement to measuring WT, many researchers have mapped microtopography (MT)—small-scale heterogeneities in the ground-surface elevation—for the purpose of upscaling point-level GHG measurements (Baird et al., 2009; Becker et al., 2008; Loisel & Yu, 2013; Nungesser, 2003; Strack et al., 2016). In addition to influencing CH_4 flux, microforms (hummocks and hollows) can also foster variations in vegetation community, hydrology, nutrient content, and temperature across peatlands (Lucieer et al., 2011; Macrae et al., 2013; Cresto Aleina et al., 2015; Acharya et al., 2015). Microtopographic observations are generally easier to acquire than WT positions, since no water wells are necessary. In addition, the temporal persistence of microforms (Nungesser, 2003) means that fewer monitoring events are required for a given site. Regardless, microform data still require detailed terrain observations, which are normally collected

with labor-intensive GPS surveys and specialized equipment (Roosevelt, 2014): a strategy that is expensive and difficult to scale (Pouliot et al., 2011; Roosevelt, 2014).

Recent developments in unmanned aerial vehicle (UAV) technology and related workflows have provided exciting new capabilities for peatland observation. UAV platforms can deliver ultrahigh-resolution imagery and 3-D point clouds (100 s of points per m^2) using consumer-grade digital cameras (Lovitt et al., 2017). In turn, these data permit the measurement of CH_4 controlling factors such as WT position (Rahman et al., 2017) and terrain (Lovitt et al., 2017) at unprecedented levels of detail, with capacity for extensive spatial coverage and flexible monitoring intervals. As a result, UAVs present researchers with novel opportunities to investigate the impacts of anthropogenic disturbances on peatland ecosystem functions.

Peatlands in the Canadian province of Alberta and elsewhere have been heavily disturbed by the construction of seismic lines for petroleum resource exploration (Pasher et al., 2013; Schneider & Dyer, 2006). Seismic lines can be extremely disruptive to low-lying peatland ecosystems, often triggering persistent changes in environmental factors such as hydrology (van Rensen et al., 2015), which may have implications on GHG release rates. Seismic lines are not limited to Alberta, occurring within various other provinces and territories of Canada as well as in other regions such as Siberia (Scott, 1994; Williams et al., 2013). Low-impact seismic (LIS) lines are widespread in Alberta and are deemed "low impact" on account of reduced clearing widths (~2–3 m) compared to legacy seismic lines (~8–10 m; Schneider & Dyer, 2006; British Columbia Oil and Gas Commission, 2016). However LIS are constructed in dense grid networks (~50 m intervals) across vast areas, and there is little evidence of enhanced recovery rates in peatlands, which are notoriously slow to recover from disturbance events (Schneider & Dyer, 2006; British Columbia Oil and Gas Commission, 2016; van Rensen et al., 2015). Few studies to date have explored the impact of LIS on physical peatland conditions (MT and hydrology) and GHG fluxes. Strack et al. (2017) provide the only related study, which investigated GHG emissions from a conventional seismic line-turned winter access road within a wooded fen in northern Alberta. Their results showed that altered ecohydrological conditions on lines can substantially increase GHG emissions, with mean CH_4 flux values measured at 479 mg CH_4 m^{-2} day^{-1}, compared to 4.9–6.3 mg CH_4 m^{-2} day^{-1} in adjacent undisturbed areas (Strack et al., 2017).

The focus of this research was twofold: first, to compare two UAV-based methods of estimating CH_4 release from a treed-bog study site in northern Alberta, Canada: (i) MT and (ii) DTW, and second, to quantify the impact of LIS lines on CH_4 release, MT, and DTW across our 61 ha study site. Our work represents the first-known spatially explicit quantification of LIS impacts on morphology, hydrology, and chemistry on peatlands in Canada.

2. Materials and Methods

2.1. Study Site

The study site is an ~61 ha portion of treed bog located roughly 35 km northeast of Peace River, Alberta (Figure 1a). Treed bogs are a type of wetland that receive water exclusively from precipitation (no input from surrounding watersheds) and accumulate organic matter (peat) on account of their low-oxygen environment (National Wetlands Working Group, 1997). Within our study site, a 3.8 ha subset area (Figure 1b) was used to assess model accuracies and generate CH_4 estimates for upscaling across the full site. The study area is heavily disturbed by resource exploration and extraction activities. A mineral-filled access road traverses the eastern portion of the site, and the center is bisected by a pipeline. However, the main focus of the present work is the dense network of ~2 m wide LIS lines, which total 16 km in length within the study area and 1.4 km in length within the subset area.

Zones disturbed by LIS appear as linear clearings through the bog and display reduced frequency of black spruce (*Picea mariana*), labrador tea (*Rhododendron groelandicum*), and small cranberry (*Oxycoccus microcarpus*), which dominate the surrounding undisturbed areas. Additionally, flattening of MT along LIS is visually apparent. In many cases, the remnants of vehicle tracks were observed along these features, having formed pools of standing water surrounded by vascular vegetation more commonly found in fen ecosystems, including willow (*Salix* spp.) and a variety of sedges. Repeated vehicle use on seismic lines in this study area was not observed, suggesting that the tracks were created during initial construction. Figure 1b shows a

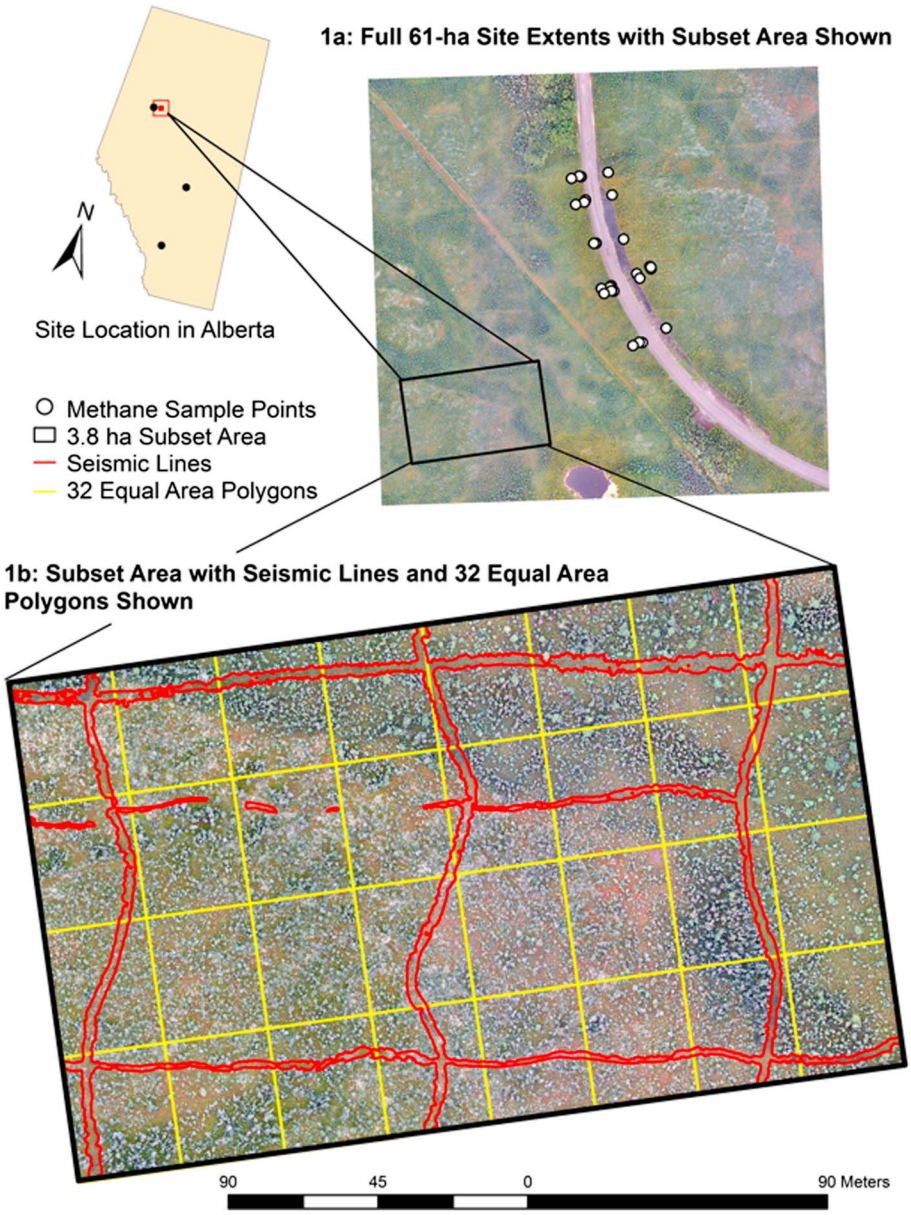

Figure 1. (a) Full study site extents and (b) subset showing equal area polygons and seismic lines used to generate CH_4 flux estimates from MT and DTW (process explained in section 2.5). Within Figure 1b, a variety of surface features can be observed including dispersed pockets of dense black spruce.

close-up view of LIS within a subset of our study area. These features were manually digitized from the orthophoto based on the observed differences in vegetation and, in many cases, the presence of vehicle tracks.

In the undisturbed portions of the bog, microforms (hummocks and hollows) are present at scales from 30 cm to 1 m diameter and height and occur in roughly equal proportions. Vegetation is typical of treed bogs within the region, with black spruce being the dominant tree species, labrador tea and small cranberry representing the majority of shrub species, and *Sphagnum* spp. (*Sphagnum fuscum*—rusty peat moss, *Sphagnum capillifolium*—acute-leaved peat moss, *Sphagnum girgensohnii*—Girgensohn's peat moss, *Sphagnum magellanicum*—midway peat moss, and *Sphagnum warnstorfii*—Warnstorf's peat moss) dominating the ground layer.

2.2. CH_4 Flux Data

Methane samples were collected at 27 points (collars) every second week over a 150 day monitoring period, which ran from May to September of 2016. Collars were permanently installed across 14 hollows and 11

hummocks in order to capture a range of data for each identified microform type. These collars were measured as part of a related study investigating the impact of a permanent access road on peatland carbon exchange, but any collars in areas specifically impacted by road construction (i.e., where vegetation had been disturbed) were not included in the present data set. Since the road has impacted hydrology at the site, some of the measurement collars were likely wetter or drier than would have occurred in undisturbed conditions, which allowed for a wider range of DTW to be considered. Therefore, although no collars were specifically located on seismic lines, they do represent the full range of MT and WT position present across the site. Prior to collecting the gas samples, a closed opaque chamber (60 × 60 × 30 cm) was fitted over each collar and sealed from the atmosphere (Tuittila et al., 2000). An internal fan mixed headspace air, and a 20 mL syringe, was used to collect gas samples at predetermined intervals (7, 15, 25, and 35 min). A thermocouple was used to determine the chamber's internal air temperature at the time each sample was collected. Gas samples were then stored in preevacuated Exetainers (Labco Ltd., UK) and shipped to the University of Waterloo for analysis. On each sampling day, four ambient gas samples were also collected to provide background CH_4 concentrations at the study site, and the WT position of wells installed beside each collar was recorded.

The CH_4 concentration of each sample was analyzed using a Shimadzu GC-2014 gas chromatograph, at the University of Waterloo, and CH_4 flux was determined from the linear change in concentration over time. Flux measurement with a poor linear relationship ($R^2 < 0.75$) was deemed indicative of chamber disturbance during measurement and was removed from the data set. These instances generally occur due to ebullition and indicate that CH_4 flux is likely poorly represented by our chamber measurements (as in other studies such as Christen et al., 2016). Therefore, flux estimates and the calculated impact of seismic lines on ecosystem CH_4 flux are likely conservative. Fluxes in which no change in CH_4 concentration was noted (i.e., change in concentration was within the precision of the gas chromatograph of 0.5 ppm) were assigned a value of zero. Approximately 10% of the data was removed following these protocols. Accepted CH_4 fluxes were then corrected for both internal chamber air temperature and chamber volume.

Flux sampling points were identified as either hummocks or hollows based on vegetation and microtopographic characteristics. On average (± standard deviation) cover of lichens, *Sphagnum* moss, shrubs, and forbs was 60 (35), 22 (28), 35 (20), and 12 (10)% at hollows and 0, 95 (17), 50 (26), and 3 (3)% at hummocks. From this segregation, the average CH_4 flux per microform (hummock versus hollow) was calculated. We then determined the relationship between CH_4 emission and DTW by applying a LOG_{10} transformation to the 150 day mean CH_4 flux data of each plot and performing a linear regression with mean WT position of each corresponding water well. Previous studies have noted that a log linear relationship exists between CH_4 flux and WT position (Bubier et al., 1993; Moore & Roulet, 1993).

2.3. Remote Sensing Observations

UAV data were acquired on 2 September 2016 using an Aeryon Skyranger fitted with an HDZoom30 RGB optical camera (20 megapixels, global shutter). The flight was completed between 9:30 a.m. and 2:00 p.m. at 110 m altitude with approximate wind speeds of 3 m/s. Data were collected continuously during flights (flight speed 4 m/s) to minimize battery replacements (three for full site coverage), with flight lines positioned to deliver 80% endlap and 60% sidelap among photographs. Ground resolution of the resulting data set was approximately 2 cm. Lighting was diffuse and low during flight operations due to persistent high cloud cover, thereby minimizing the amount of shadow in the imagery. It is worth noting that small pools of standing water were dispersed across the site resulting from very wet conditions leading up to flight operations. These pools may have influenced UAV product accuracies due to increased surface homogeneity and reflectivity, though accuracies of the resultant dense point cloud and digital surface models were deemed sufficient to proceed with secondary analyses.

2.4. Classification of Terrain (Microtopography)

The workflow used to generate a classified MT surface is provided in the supporting information associated with this publication (Figure S1). From the aerial data, a dense point cloud comprised only of ground points, which we call the ground dense point cloud (gDPC), was generated as per Lovitt et al. (2017). Accuracies of the gDPC were estimated by PhotoScan (Version: 1.2.4) as ~0 cm (*x*,*y*) and 21 cm (*z*). Nearest-neighbor interpolation was applied to the gDPC in Environmental Systems Research Institute ArcMap (Version: 10.3.1) to

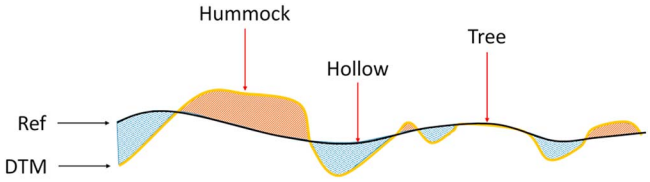

Figure 2. Process of producing the microtopography surface by subtracting the reference surface (Ref) from the digital terrain model (DTM). Areas above Ref are considered hummocks (brown), areas below are considered hollows (light blue), and areas which are masked are assigned the class "Trees."

generate the digital terrain model (DTM). Using ENVI (Version 5.1), we then applied a mask, buffered by 18 pixels, over treed areas, followed by a low-pass filter (window size 2 m) to generate a reference surface (Ref) representing general site slope. The purpose of buffering the tree mask was to ensure that vegetation edge points (i.e., points falling on the boundary between terrain and tree, as per Lovitt et al., 2017) were excluded from the low-pass filter calculation. The purpose of excluding these points was to avoid artificially increasing ground-surface elevations in areas where points represented vegetation rather than ground. A window size of 2 m was selected for the low-pass filter after comparison with window sizes of 1, 1.5, and 3 m. In order to ensure ENVI was excluding masked areas (assigned 0 value) in the averaging window calculation, we applied a custom IDL script, which forced ENVI to average pixels with nonzero values only. Finally, after generating Ref, we subtracted it from the DTM [DTM-Ref] to generate a MT elevation surface (Figure 2).

We classified the MT surface using a simple, pixel-based density slicing approach in ENVI. A total of three classes were identified across the site: (i) hummocks, (ii) hollows, and (iii) trees. The classification specified hummocks >0, hollows <0, and trees = 0 (masked). The approach was based on the assumption that areas taller than the average elevation of the surrounding peatland (positive MT surface values) corresponded to hummocks, while areas below the average elevation (negative MT surface values) corresponded to hollows (Figure 2).

Classification accuracy was assessed by generating a confusion matrix using 105 validation points collected in the field. Samples were selected using a stratified-random sampling strategy, and observed locations were surveyed using a Trimble R4 real-time kinematic Global Navigation Satellite System. In addition to this ground data, 50 random points representing tree pixels were selected for assessment of the tree class. Results of this classification are summarized in Table 1. The overall accuracy of the classification was 84% (kappa: 0.76). This classification performed well overall, though it resulted in a slight over-representation of hollows (86% producer's accuracy versus 77% user's accuracy) and a slight under-representation of trees (92% producer's accuracy versus 100% user's accuracy) across the site. However, there appears to be no bias in the classification of hummocks (75% producer's accuracy versus 77% user's accuracy). The majority of errors in distinguishing hummocks and hollows were found to occur in cases where the target microform was within ±5 cm of the reference surface, an area we define as the microform "transition zone." The accuracy of the classification was comparable to results reported in similar studies (Lehman et al., 2016) and was therefore deemed acceptable for use in estimating CH_4 emissions and disturbance related changes in MT.

2.5. Generating the Depth to Water Surface (DTW) Surface

The DTW surface was generated using the methods described by Rahman et al. (2017). In their workflow, areas of stable open water were first classified using a decision-tree classification scheme. From among the resulting classified pixels, spatially distributed samples of open water were selected, and their elevations interpolated via ordinary kriging to obtain the height of the WT in meters above mean sea level. The groundwater-level surface was then subtracted from the DTM to obtain DTW. The accuracy of the DTW surface was assessed as per Rahman et al. (2017). Validation of the DTW surface was completed by comparing modeled values against field data collected at five wells within the study site. The results of this comparison indicated an root-mean-square error (RMSE) of the DTW surface in the study area subset of 11.3 cm.

Since WT fluctuates throughout the year, we needed to adjust the DTW surface estimated at the date of the UAV flight on 2 September in order to reflect the mean value of DTW across our flux monitoring period from May to September. True point measures of DTW were observed at 37 water wells across the study area by field personnel every two weeks. We selected the well that was located closest to our 3.8 ha subset area and averaged all measurements to

Table 1
Confusion Matrix of Pixel-Based Density Slicing Classification Approach (Overall Accuracy = 84%; Kappa = 0.76)

		Reference				User's Accuracy
	n = 155	Hummock	Hollow	Trees	Total	(%)
Predicted	Hummock	40	8	4	52	77
	Hollow	13	44	0	57	77
	Trees	0	0	46	46	100
	Total	53	52	50	155	
	Producer's Accuracy (%)	75	86	92		

determine the mean DTW in the well over the 150 day monitoring period. We then compared this value with that estimated from our UAV model at the well's location (collected as part of the terrestrial survey via real-time kinematic Global Navigation Satellite System). This comparison revealed that the mean DTW, as calculated from the water well data, was 4.8 cm lower than the DTW position estimated by the UAV model for 2 September. As a result, we lowered the DTW model by 4.8 cm to better reflect the seasonal average. This adjustment assumes that WT fluctuates consistently across the site and that averaging the collected data from one sampling point is sufficient to estimate mean WT position across the larger area.

2.6. Estimating CH_4 Flux

The subset area was divided into 32 equal-area quadrats (~1,189 m^2 each) to allow for a statistical analysis of flux estimates within each quadrat (Figure 1b). Both LIS and undisturbed portions of the treed bog occurred within the subset area. LIS were clearly distinguishable from undisturbed bog in the high-resolution UAV orthophoto and were manually digitized in Environmental Systems Research Institute ArcMap 10.3.1 for the entire 61 ha study area. We clipped the MT and DTW layers using seismic-line boundaries to divide the study site into two categories: undisturbed and disturbed. CH_4 emissions were then estimated from each category (undisturbed: MT and DTW, disturbed: MT and DTW) for each of the 32 polygons.

To estimate CH_4 fluxes from MT, the percent-area coverage of hummock, hollow, and tree (undisturbed) was calculated and multiplied by the corresponding average fluxes of 13.3, 34.5, and 24.3 mg CH_4 m^{-2} day^{-1}. The standard errors of these fluxes were estimated as 3.8, 9.5, and 0.09 mg CH_4 m^{-2} d^{-1}, respectively. As CH_4 fluxes were not directly measured in areas below trees, we assigned average CH_4 values to treed areas. Based on field observations of microtopographic conditions below trees, no discernable pattern in microform occurrence in these areas was identified, so applying an average flux value was considered appropriate. This approach involved calculating the average flux for undisturbed and disturbed portions of the polygon, estimated exclusively by the areal coverage of classified hummocks and hollows in these areas. Since this method estimated greater CH_4 emission within disturbed areas (higher occurrence of hollows), a slightly higher average flux value of 26.1 mg CH_4 m^{-2} day^{-1} was used for trees in these areas. The standard error of this flux was estimated as 0.3 mg CH_4 m^{-2} day^{-1}.

To estimate CH_4 flux from DTW, the log linear equation developed in section 2.2 was applied to the DTW surface. This produced a CH_4 surface with flux values across the site at 2 cm resolution. The same buffered tree mask was then applied to the DTW surface to ensure flux estimates between the DTW and MT surface were comparable. Similar to the MT surface, treed areas were assigned an average flux value based upon their surrounding conditions; that is, Trees [undisturbed]: 12.2 mg CH_4 m^{-2} d^{-1} and Trees [disturbed]: 27.5 mg CH_4 m^{-2} day^{-1} with a corresponding standard error of 1.0 and 3.6 mg CH_4 m^{-2} day^{-1}.

3. Results

3.1. Estimating CH_4 Flux

The LOG_{10} approach was found to improve both the normality of the CH_4 flux data distribution and residual errors of the regression. Across all sampling plots, the relationship between CH_4 flux and WT position ($p < 0.01$; $R^2 = 0.28$; Figure 3) was described by the following equation:

$$\log_{10}(CH_4) = 0.0305^{*}\text{WTposition} + 1.5257 \quad (1)$$

3.2. Modeled Surfaces

The two modeled surfaces (MT and DTW) were used to predict CH_4 emissions across the study site following the methods described in section 2. Figure 4 displays these surfaces as modeled over a small subsection of the study area.

3.3. Seismic Line Impacts on MT and DTW

Mean ground elevations were significantly different between undisturbed and disturbed areas ($p < 0.01$), with seismic lines occurring 2.2 cm lower on average relative to undisturbed peat (RMSE: 2.6 cm). Additionally, an overall flattening of microtopographic features was noted along LIS (MT), with the majority of microforms existing within ±5 cm of Ref. By comparison, greater variation in ground-surface elevations was noted in undisturbed areas, specifically an increased occurrence of tall hummocks (i.e., ground >10 cm of Ref).

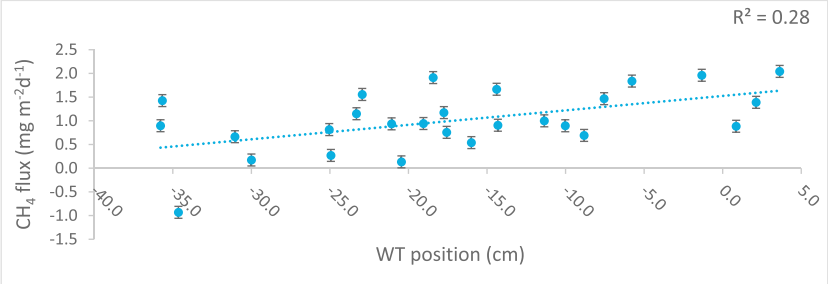

Figure 3. Relationship between LOG_{CH4} (mg m^{-2} day^{-1}) and water table position (cm), where water table located below ground surface is given a negative value. The error bars indicate the standard error of LOG_{CH4} values (±0.13).

Ground elevations in undisturbed areas (32 total polygons) ranged from −74 cm below to +97 cm above Ref, with a mean value of 0.6 cm. Comparatively, elevations in disturbed areas (27 total polygons) ranged from −64 to +64 cm, with a mean value of −1.5 cm (Table 2). This translates to a 46 cm reduction in the average microform elevation range within seismic lines.

A near-equal frequency of hummock versus hollow occurrence was noted in undisturbed areas (51.8% hollow coverage). However, an increase in hollow prevalence (60.8% coverage) was observed along seismic lines (Table 2).

Significant differences in DTW were found to exist between seismic lines and undisturbed peatland areas ($p < 0.01$). In undisturbed areas, DTW ranged from 159 cm below to 71 cm above ground surface, with a mean value of 17.5 cm below surface (Table 2). Along seismic lines, DTW ranged from 81 cm below to 39 cm above ground surface, with a mean value of 2.1 cm below the surface. Comparing average values suggests that little difference exists in maximum DTW values between undisturbed areas (24 cm) and disturbed areas (21 cm). However, there were clear differences in the calculated average minimum DTW values (−95 cm versus -40 cm respectively). This indicates that a shallower WT position exists along seismic lines (average difference 15.4 cm; RMSE: 17.5 cm).

3.4. CH4 Flux Estimates and Quantification of Seismic Line Impacts

Table 3 summarizes partial (undisturbed versus disturbed) and total (undisturbed + disturbed) CH_4 flux estimates for the study site as calculated by both MT and DTW, as well as estimated increase (%) of CH_4 along seismic lines. Significant differences were noted between the MT and DTW surfaces when predicting CH_4 flux in undisturbed areas ($p < 0.01$) but not along seismic lines ($p = 0.454$). Total CH_4 for the 3.8 ha study site over the 150 day flux monitoring period was estimated as 124 kg by the MT surface, and 76 kg by the DTW surface, resulting in the MT surface estimating +48 kg CH_4 more than the DTW. The correlation between the two surfaces' estimates in undisturbed areas was slightly lower (0.55) than that observed in disturbed areas (0.69). Methane emissions are predicted to increase substantially (MT: +20%, DTW: +120%) on seismic lines relative to undisturbed peatland. Results of the statistical analysis indicate that these differences are significant ($p < 0.01$) in both surfaces (MT and DTW).

To estimate CH_4 flux per linear kilometer of LIS, we multiplied predicted CH_4 flux (in kg per m^2 day^{-1}) by the estimated line width (2 m) and length (1,000 m). Both MT and DTW surfaces estimate approximately 0.050 kg CH_4 day^{-1} per linear kilometer of LIS (MT: 0.052 kg CH_4 day^{-1}, DTW: 0.054 kg CH_4 day^{-1}). This translates to an increase between 0.011 and 0.027 kg CH_4 day^{-1} per linear kilometer of LIS. These values can be adjusted to represent older, legacy lines of varying widths as desired.

Table 4 presents estimates of CH_4 flux across the entire 61 ha study site. Excluding other disturbance features (pipeline and road) LIS account for approximately 5.2% of the total site coverage. Assuming the site had 0% seismic line disturbance, total site CH_4 emission estimated over the 150 day monitoring period is predicted to be between 1,130 kg CH_4 (DTW) and 1,990 kg CH_4 (MT). The standard error for these values is estimated to be 30 and 13 kg CH_4, respectively. Adjusting these predictions to include 5.2% LIS disturbance, total CH_4 emission estimates increase to 1,200 kg CH_4 (DTW) and 2,010 kg CH_4 (MT), with standard errors of 15 and 2 kg CH_4, respectively. This translates to an absolute total site CH_4 emission increase at the 61 ha site over the 150 day monitoring period of approximately 70 and 20 kg, respectively.

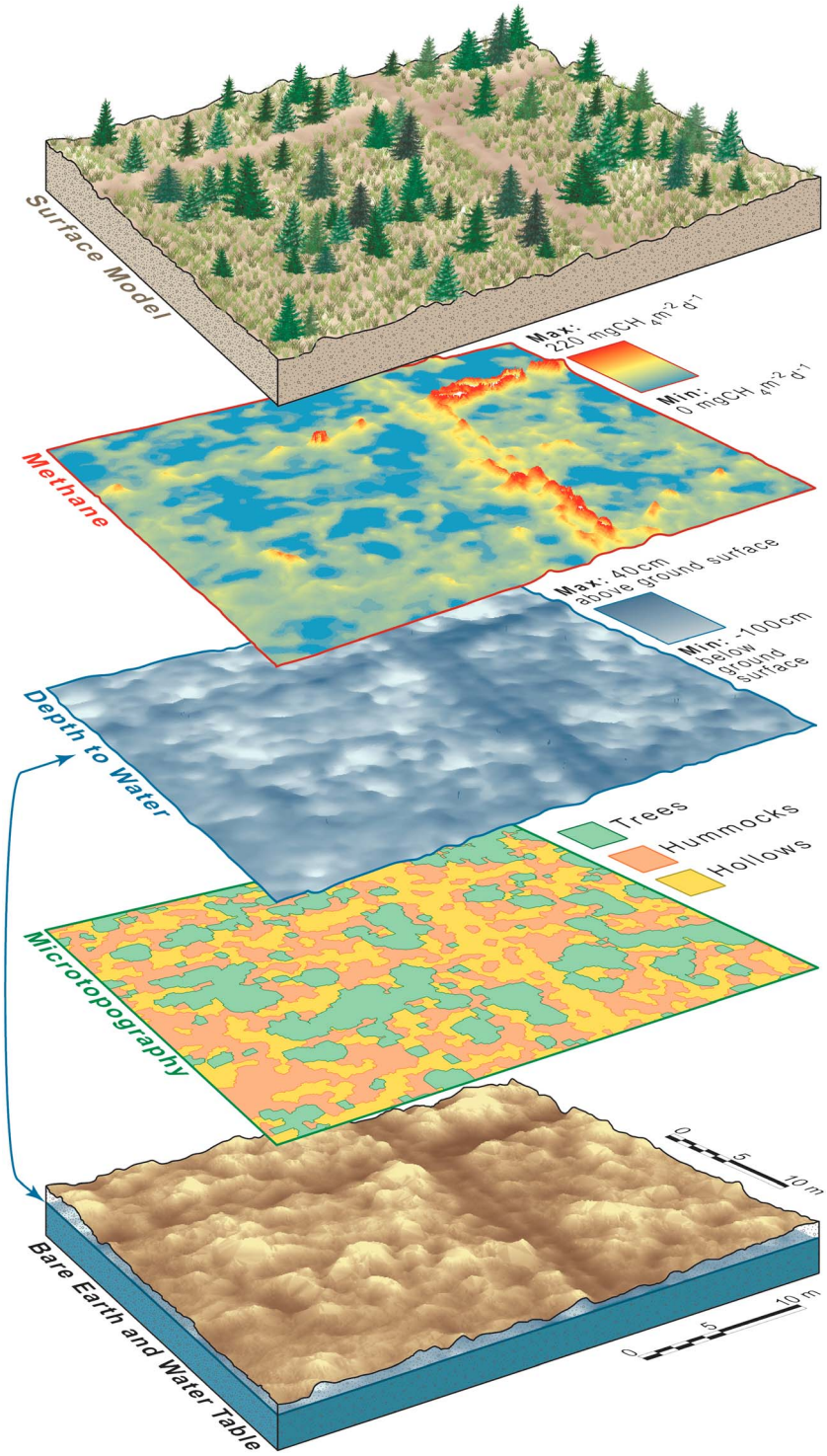

Figure 4. Graphical visualization of digital surfaces generated from the input surface model (shown at top of stack). Surfaces include the bare earth and WT, MT, DTW, and CH_4. DTW is shown in centimeter where depths below ground surface are negative; CH_4 is shown in mg CH_4 m^{-2} day^{-1}. The DTW surface was derived from the bare earth and WT surfaces; the arrow shows this link to the WT position below ground surface. Figure prepared by Robin Poitras and Julie Lovitt at the University of Calgary.

Using the 0% disturbance-site flux values, we performed a sensitivity analysis of calculated CH_4 emissions across the study site over the 150 day monitoring period, based on the errors documented for both surfaces (11.3 cm RMSE for DTW; 84% for MT). The DTW surface was regenerated twice: once lower (DTW minus

Table 2
Summary Table Showing Absolute and Average Differences in Mcroform Heights, Percent Coverage, and Measured Depth to Water Between Undisturbed and Disturbed Areas

			Undisturbed (32 polygons)	Disturbed (27 polygons)
Microform height (cm)	Absolute	Minimum	−74	−64
		Maximum	97	64
		Range	171	128
	Average	Minimum	−48	−30
		Maximum	69	41
		Range	117	71
		Mean	0.6	−1.5
		Hummock/hollow coverage (%)	48.2/51.8	39.2/60.8
Depth to water (cm)	Absolute	Minimum	−159	−81
		Maximum	71	39
		Range	230	120
	Average	Minimum	−95	−40
		Maximum	24	21
		Range	119	61
		Mean	−17.5	−2.1

11.3 cm) and once higher (DTW plus 11.3 cm) based on reported RMSEs. These adjustments produced estimated CH_4 fluxes ranging from 960 (DTW minus 11.3 cm) to 2,200 kg CH_4 61 ha^{-1} 150 day^{-1} (DTW plus 11.3 cm), revealing the estimated uncertainty in our DTW generated CH_4 predictions. We did a similar analysis for the fluxes estimated from the MT surface, both increasing (plus 16%) and decreasing (minus 16%) the proportion of hummocks to hollows, based on reported accuracies. These adjustments produced estimated CH_4 fluxes ranging from 1,480 (proportion of hummocks plus 16%) to 2,200 kg CH_4 61 ha^{-1} 150 day^{-1} (proportion of hollows plus 16%). Again, we interpret this as an estimate of uncertainty in our MT generated CH_4 predictions. The sensitivity analyses reveal greater uncertainty in CH_4 estimates arising from the DTW surface (960–2,200 kg CH_4 61 ha^{-1} 150 day^{-1}) than the MT surface (1480–2,200 kg CH_4 61 ha^{-1} 150 day^{-1}).

4. Discussion

We conducted a thorough comparison of peatland microtopographic and DTW characteristics across our study area to determine how seismic lines have impacted these key environmental factors. Results of this assessment indicate that LIS lines at the study site caused an overall flattening of microforms, increase in hollow frequency, and decreased the mean ground elevations by 2 cm (RMSE: 2.6 cm). These same disturbances decreased mean DTW by 15.5 cm. By comparison, a study investigating permafrost-related impacts in Canada's Northwest Territories showed that seismic lines on permafrost peatlands produced ground subsistence between 3 and 53 cm (Williams et al., 2013). While these dramatic results are caused at least in part due to altered permafrost regimes along seismic lines, they reflect the trends observed in our analysis: LIS lines stand out from the surrounding peatland as lower, wetter, and flatter areas. Assuming that our study site is indicative of typical treed bog conditions, these findings can partially explain the lack of successful ecosystem recovery (i.e., restoration of ground surface, hydrological, and vegetation conditions comparable to predisturbance) along linear features within the western Canadian Boreal region. van Rensen et al. (2015) indicated that wetter (flooded) areas are less likely to establish new Sphagnum moss communities, an important genus in natural hummock formation. This suggests that LIS lines within our study site, and those in comparable disturbed peatlands, are highly unlikely to recover without the pursuit of active restoration designed to recreate suitable surface conditions.

Furthermore, the results of our CH_4 flux estimates indicate the strength of the link between lower, wetter peatland conditions, as found along LIS, and significantly increased CH_4 emissions. Both MT and DTW predict CH_4 release increases between 20% (MT) and 120% (DTW) along LIS (2 m width) compared to adjacent undisturbed areas. Logically, it follows that wider conventional lines, such as those constructed in the mid-1950s, would produce even higher CH_4 emissions per linear kilometer. Considering these wider lines have been linked to other altered environmental conditions, including light exposure and surface temperatures

Table 3
Predicted CH_4 Emissions of 3.8 ha Subset Study Site Over 150 Day Monitoring Period and Estimated Increase (per ha) Due to Seismic Line Disturbance

		MT surface (standard error)	DTW surface (standard error)
Undisturbed	Total estimated CH_4 flux (kg day^{-1})	0.759 (0.0003)	0.433 (0.0006)
	Total area (ha)	3.78	3.78
	Avg predicted flux (kg ha^{-1} day^{-1})	0.216 (0.1)	0.123 (0.3)
Disturbed	Total estimated CH_4 flux (kg day^{-1})	0.070 (0.0003)	0.072 (0.0004)
	Total area (ha)	0.269	0.267
	Avg predicted flux (kg ha^{-1} day^{-1})	0.261 (0.3)	0.270 (3.0)
Total Site	CH_4 increase per ha due to disturbance	20%	120%
	Percent of site disturbed	7%	7%
	Total predicted flux for site (kg 3.8 ha^{-1} 150 day^{-1})	124	76

Table 4
Estimated Total CH_4 Emission Across 61 ha Study Site (as per Figure 1a) and Predicted Increase Over 150 day Monitoring Period Due to Seismic Line Disturbance

	Undisturbed	Disturbed
Areal coverage	94.8%	5.2%
MT flux (kg ha^{-1} day^{-1})	0.216	0.261
DTW flux (kg ha^{-1} day^{-1})	0.123	0.270
	MT surface	DTW surface
Total predicted flux in undisturbed areas (kg ha^{-1} day^{-1})	1.25	0.71
Total predicted flux in disturbed areas (kg ha^{-1} day^{-1})	0.08	0.09
Theoretical total predicted flux of site (%coverage of LIS = 0) (kg ha^{-1} day^{-1})	1.32	0.75
Actual total predicted flux of site (%coverage of LIS = 5.2) (kg ha^{-1} day^{-1})	1.33	0.80
Absolute total site CH_4 increase due to disturbance (kg 61 ha^{-1} 150 day^{-1})	20	70

(Dabros et al., 2017), these increases in CH_4 emission may be exponential, and the cumulative emission of unreclaimed LISs over their lifespan is likely to be highly significant.

In this study, MT and DTW were modeled from UAV data with good results (MT: 84% overall accuracy, DTW: 11.3 cm RMSE), though uncertainties within these layers persist. Our sensitivity analyses reveal these uncertainties to produce greater variability in CH_4 output from the DTW surface. This is perhaps predictable, given the simpler nature by which CH_4 estimates are upscaled with the MT surface, using a small number of averaged microform fluxes. However, it also reflects the fact that the log linear equation (1) of the DTW approach is highly sensitive to the quality of input water-level data; small errors in estimated WT position may produce large uncertainty in CH_4 predictions. Unfortunately, we had insufficient flux data to perform an accuracy assessment of CH_4 estimates: something that should be pursued in future research.

Lacking a proper model validation, we assume that the more technically complex DTW surface is more representative of real-world conditions in undisturbed areas due to the higher spatial resolution of CH_4 estimates. This is in line with previous studies that indicate simple classifications are likely to overestimate or underestimate CH_4 emission (Hartley et al., 2015; Lehmann et al., 2016). However, there was no significant difference in estimates from either surface along seismic lines. The higher estimation of the MT surface within undisturbed areas is likely due to the wide range of flux rates reported across microforms of differing heights (hummocks) and depths (hollows). We suggest that including additional classes of microforms, such as lawns, or incorporating some detail of vegetation community characteristics may address this issue by accounting for greater variability in both microforms and CH_4 emission rates within undisturbed peatland areas (Bubier et al., 1993). Furthermore, this may overcome classification issues in differentiating hummocks from hollows as the majority of these errors were found to occur in the transition zone, the area between clearly identifiable microforms (±5 cm of Ref). Alternatively, a Lawn class could be created to capture areas within the transition zone. Bubier et al. (1993) define lawns as areas that are relatively flat compared to the surrounding peatland surface. In this case, areas within the identified transition zone would fit the description of lawns as they are within 5 cm of the mean peatland surface elevation.

4.1. Potential Sources of Errors

As described in Lovitt et al. (2017) and Rahman et al. (2017) numerous external factors, such as weather conditions during UAV operations and input model accuracies (i.e., DTM, water level surface), may have affected the accuracy of our results. These factors were addressed in their respective manuscripts and will not be discussed further.

The microtopographic classification method applied in this study could be improved. Due to the slight over representation of hollows, the MT surface likely overestimates CH_4 flux in undisturbed areas and comparatively underestimates the impact of seismic lines. Similarly, the inclusion of vegetation border points during DTM generation caused us to apply an 18 pixel buffer to the tree mask, which likely removed useful terrain pixels from the MT model. Predicting CH_4 emission from the MT model was limited by a lack of CH_4 measurements across a variety of microform heights. As a result, average flux values were applied to only three microform classes (hummocks, hollows, and trees), which likely overestimated flux from undisturbed areas.

Although CH_4 estimates from the DTW surface were anticipated to be more accurate than the MT surface, the reported R^2 value (0.28) of the LOG(CH_4) linear equation (1) may explain a degree of uncertainty in the results.

While this R^2 value is comparable to similar studies (Moore & Roulet, 1993: $R^2 = 0.332$), others have reported stronger relationships between peatland CH_4 flux and WT position (Bubier et al., 1993: $R^2 = 0.649$; Shannon & White, 1994: $R^2 = 0.58$, Sundh et al., 1994: $R^2 = 0.50$, Bubier, 1995: $R^2 = 0.74$), Therefore, expanding the CH_4 data set (spatially or temporally) may strengthen the relationship between CH_4 flux and WT position and improve CH_4 estimates from the DTW surface. Conversely, this R^2 value may indicate that other environmental factors have greater influence on CH_4 generation and emission at this study site. For example, previous studies indicate that soil temperature may influence bog CH_4 flux (van Winden et al., 2012), and vegetation type is often a strong predictor of peatland CH_4 flux (Bubier, 1995; Couwenberg et al., 2011).

The lack of CH_4 measurements within disturbed and undisturbed portions of the subset area is another potential source of error. For the purposes of this study, we assumed that the relationship between CH_4 flux and WT position within our subset was comparable to that modeled from data collected up to 200 m away. This assumption was based on the fact that the subset area and all flux measurement points existed within the same treed bog ecosystem. However, without proper validation, it is unclear whether this assumption was well founded or not.

It was beyond the scope of this paper to investigate other disturbance features present at the study site (pipeline and road). However, these features likely have similar impacts on peatland hydrology and MT, and we recommend future research on how they may alter peatland CH_4 release. Moreover, peat composition and biogenic gas distribution are anticipated to be comparable across the entire 61 ha study site, which may not be the case if woody debris or confining layers, such as peat with low permeability, vary (Comas et al., 2014). Therefore, these methods of estimating CH_4 emissions across large areas may need to be modified by site-specific criteria prior to application.

5. Conclusions

The primary objective of this research was to use UAV data to quantify the impact of seismic lines on peatland CH_4 emissions, MT, and DTW within a boreal treed bog in northern Alberta, Canada. From this investigation, we determined that seismic lines have significant impacts on the peatland ecosystem, causing overall flattening of MT and decreasing DTW, resulting in significant increases in CH_4 release. Based on this assessment, and the knowledge that seismic lines are widespread within the western Canadian Boreal region, we suggest that these linear disturbances should be included in land use change GHG emission estimation to avoid underreporting at the national scale. Furthermore, due to the noted degree of MT and DTW disturbance, we posit that active restoration will likely be necessary to achieve recovery of vegetation and ecosystem function along LIS. Additional data are required to properly validate the CH_4 flux estimates and determine which UAV method is superior; however, we believe that the relationships presented here (significant increase in CH_4 emission along seismic lines) are valid based upon the assessment of altered physical parameters (MT and DTW).

This research represents an initial attempt to determine how LIS have altered boreal peatland carbon balance and storage functions at a single treed bog in northern Alberta. However, peatlands are incredibly diverse ecosystems and we encourage additional studies building upon our methods to more thoroughly investigate hydrological impacts and/or to assess similar disturbance features within different peatland types. Moreover, assessing the impact of mineral-filled linear disturbances, such as pipeline right of ways and resource roads, would be beneficial. Additionally, it would be useful to upscale these findings to the regional level and/or adjust national GHG estimates to include disturbance features, especially considering key points in the current provincial government's Climate Leadership Plan have been identified as reducing CH_4 emissions by 45% by 2025, and improving management of industry GHG emissions (Government of Alberta, 2017). On the broader scale, the methods described in this paper may be useful in assessing the impact of other types of small-scale disturbances, such as drainage ditches, within peatland ecosystems across the globe.

Acknowledgments
Research funding was provided by Emissions Reduction Alberta (grant BI40020) and Shell Canada Ltd, and a NSERC Discovery Grant to McDermid. We also thank Shell Canada for site access and logistical support, UAV Geomatics, Melanie Bird (NAIT), Christina Braybrook (UofC), Annie He (UofC), and the University of Waterloo for assisting with project design and facilitating field data collection, as well as Robin Poitras (UofC) for his assistance with figure generation. We would like to extend a sincere thank you to the anonymous reviewers whose comments significantly improved this article. The authors declare no conflict of interest. The funding sponsors had no role in the design of the study; in the collection, analyses, or interpretation of data; in the writing of the manuscript, and in the decision to publish the results. Select supporting information is available online (https://doi.org/10.5683/SP/AZ8J0C).

References

Acharya, S., Kaplan, D. A., Casey, S., Cohen, M. J., & Jawitz, J. W. (2015). Coupled local facilitation and global hydrologic inhibition drive landscape geometry in a patterned peatland. *Hydrology and Earth System Sciences*, *19*(5), 2133–2144. https://doi.org/10.5194/hess-19-2133-2015

Baird, A. J., Belyea, L. R., & Morris, P. J. (2009). Upscaling of peatland-atmosphere fluxes of methane: Small-scale heterogeneity in process rates and the pitfalls of "bucket-and-slab" models. In A. J. Baird, et al. (Eds.), *Carbon Cycling in Northern Peatlands, Geophysical Monograph* (pp. 37–53). Washington, DC: American Geophysical Union.

Becker, T., Kutzbach, L., Forbrich, I., Schneider, J., Jager, D., Thees, B., & Wilmking, M. (2008). Do we miss the hot spots?—The use of very high resolution aerial photographs to quantify carbon fluxes in peatlands. *Biogeosciences*, *5*(5), 1387–1393. https://doi.org/10.5194/bg-5-1387-2008

British Columbia Oil and Gas Commission (2016). Natural recovery on low impact seismic lines in Northeast British Columbia (BCIP-2016-18). Prepared by: Golder Associates. Report No. 1654243. Retrieved from http://www.bcogris.ca/sites/default/files/bcip-2016-18-natural-recovery-lis-final-report-golderexplor.pdf

Bubier, J. (1995). The relationship of vegetation to methane emission and hydrochemical gradients in northern peatlands. *Journal of Ecology*, *83*(3), 403–420. https://doi.org/10.2307/2261594

Bubier, J., Costello, A., & Moore, T. R. (1993). Microtopography and methane flux in boreal peatlands, northern Ontario, Canada. *Canadian Journal of Botany*, *71*(8), 1056–1063. https://doi.org/10.1139/b93-122

Christen, A., Jassal, R. S., Black, T. A., Grant, N. J., Hawthorne, I., Johnson, M. S., et al. (2016). Summertime greenhouse gas fluxes from an urban bog undergoing restoration through rewetting. *Mires and Peat*, *17*(3), 1–24.

Comas, X., Kettridge, N., Binley, A., Slater, L., Parsekian, A., Baird, A. J., et al. (2014). The effect of peat structure on the spatial distribution of biogenic gases within bogs. *Hydrological Processes*, *28*(22), 5483–5494. https://doi.org/10.1002/hyp.10056

Couwenberg, J., & Fritz, C. (2012). Towards developing IPCC methane 'emission factors' for peatlands (organic soils). *Mires and Peat*, *10*(3), 1–17.

Couwenberg, J., Thiele, A., Tanneberger, F., Augustin, J., Bärish, S., Dubovik, D., et al. (2011). Assessing greenhouse gas emissions from peatlands using vegetation as a proxy. *Hydrobiologia*, *674*(1), 67–89. https://doi.org/10.1007/s10750-011-0729-x

Cresto Aleina, F., Runkle, R. K., Kleinen, T., Kutzbach, L., Schneider, J., & Brovkin, V. (2015). Modeling micro-topographic controls on boreal peatland hydrology and methane fluxes. *Biogeosciences*, *12*(19), 5689–5704. https://doi.org/10.5194/bg-12-5689-2015

Dabros, A., Hammond, H. E. J., Piinzon, J., Pinno, B., & Langor, D. (2017). Edge influence of low-impact seismic lines for oil exploration on upland forest vegetation in northern Alberta (Canada). *Forest Ecology and Management*, *400*, 278–288. https://doi.org/10.1016/j.foreco.2017.06.030

Government of Alberta (2017). Climate leadership plan: Reducing methane emissions. [online content]. Retrieved from https://www.alberta.ca/climate-leadership-plan.aspx

Hartley, I. P., Hill, T. C., Wade, T. J., Clement, R. J., Moncrieff, J. B., Prieto-Blanco, A., et al. (2015). Quantifying landscape-level methane fluxes in subarctic Finland using a multiscale approach. *Global Change Biology*, *21*(10), 3712–3725. https://doi.org/10.1111/gcb.12975

IPCC (2013). Climate Change 2013: The Physical Science Basis. Contribution of Working Group I to the Fifth Assessment Report of the Intergovernmental Panel on Climate Change. In T. F. Stocker, et al. (Eds.) (pp. 33–118). Cambridge, UK and New York: Cambridge University Press.

IPCC (2014a). Topic 3: Greenhouse Gas Metrics and Mitigation Pathways. In Core Writing Team, R. K. Pachauri, & L. A. Meyers (Eds.), *Climate Change 2014: Synthesis Report. Contribution of Working Groups I, II and III to the Fifth Assessment Report of the Intergovernmental Panel on Climate Change* (87 pp.). Geneva, Switzerland: IPCC.

IPCC (2014b). Drivers, trends and mitigation. In O. Edenhofer, et al. (Eds.), *Climate Change 2014: Mitigation of Climage Change. Contribution of Working Group III to the Fifth Assessment Report of the Intergovernmental Panel on Climate Change* chap. 5, pp. 351–411). Cambridge, UK and New York: Cambridge University Press.

Kellner, E., Waddington, J. M., & Price, J. S. (2005). Dynamics of biogenic gas bubbles in peat: Potential effects on water storage and peat deformation. *Water Resources Research*, *19*, GB1003. https://doi.org/10.1029/2004GB002330

Lee, D. R., & Cherry, J. A. (1979). A field exercise on groundwater flow using seepage meters and mini-piezometers. *Journal of Geological Education*, *27*(1), 6–10. https://doi.org/10.5408/0022-1368-27.1.6

Lehmann, J. R. K., Munchberger, W., Knoth, C., Blodau, C., Nieberding, F., Prinz, T., et al. (2016). High-resolution classification of south Patagonian peat bog microforms reveals potential gaps in up-scaled CH4 fluxes by use of unmanned aerial system (UAS) and CIR imagery. *Remote Sensing*, *8*, 1–19.

Loisel, J., & Yu, Z. (2013). Surface vegetation patterning controls carbon accumulation in peatlands. *Geophysical Research Letters*, *40*, 5508–5513. https://doi.org/10.1002/grl.50744

Lovitt, J., Rahman, M. M., & McDermid, G. J. (2017). Assessing the value of UAV photogrammetry for characterizing terrain in complex peatlands. *Remote Sensing*, *9*(12), 715. https://doi.org/10.3390/rs9070715

Lucieer, A, Robinson, S., & Turner, D. (2011). Unmanned aerial vehicle (UAV) remote sensing for hyperspatial terrain mapping of Antarctic Moss beds based on Structure from Motion (SfM) point clouds. In *Proceeding of the 34th International Symposium on Remote Sensing of Environment, Sydney, Australia, (January 2008)* (pp. 1–4).

Macrae, M. L., Devito, K. J., Strack, M., & Waddington, J. M. (2013). Effect of water table drawdown on peatland nutrient dynamics: Implications for climate change. *Biogeochemistry*, *112*(1–3), 661–676. https://doi.org/10.1007/s10533-012-9730-3

Moore, T., & Roulet, N. T. (1993). Methane flux: Water table relations in Nothern wetlands. *Geophysical Research Letters*, *20*(7), 587–590. https://doi.org/10.1029/93GL00208

Munir, T. M., Xu, B., Perkins, M., & Strack, M. (2014). Responses of carbon dioxide flux and plant biomass to water table drawdown in a treed peatland in Northern Alberta: A climate change perspective. *Biogeosciences*, *11*(3), 807–820. https://doi.org/10.5194/bg-11-807-2014

National Wetlands Working Group (1997). In B. G. Warner & C. D. A. Rubec (Eds.), *The Canadian Wetland Classification System* (2nd ed., 68 pp.). Waterloo, ON, Canada: Wetlands Research Centre, University of Waterloo.

Nungesser, M. K. (2003). Modelling microtopography in boreal peatlands: Hummocks and hollows. *Ecological Modelling*, *165*(2-3), 175–207. https://doi.org/10.1016/S0304-3800(03)00067-X

Parish, F., Sirin, A., Charman, D., Joosten, H., Minayeva, T., Silvius, M., et al. (2008). Assessment on peatlands, biodiversity and climate change: Main Report. Kuala Lumpur and Wageningen. https://doi.org/10.1017/CBO9781107415324.004

Pasher, J., Seed, E., & Duffe, J. (2013). Development of boreal ecosystem anthropogenic disturbance layers for Canada based on 2008 to 2010 Landsat imagery. *Canadian Journal of Remote Sensing*, *39*(1), 42–58. https://doi.org/10.5589/m13-007

Pouliot, R., Rochefort, L., & Karofeld, E. (2011). Initiation of microtopography in revegetated cutover peatlands. *Applied Vegetation Science*, *14*(2), 158–171. https://doi.org/10.1111/j.1654-109X.2010.01118.x

Rahman, M. M., Lovitt, J., McDermid, G. J., Strack, M., & Xu, B. (2017). Mapping peat groundwater table dynamics using unmanned aerial vehicle and photogrammetric techniques. *Remote Sensing*, *9*(12), 1057. https://doi.org/10.3390/rs9101057

Roosevelt, C. (2014). Mapping site site-level microtopography with Real-Time Kinematic Global Navigation Satellite Systems (RTK GNSS) and unmanned aerial vehicle photogrammetry (UAVP). *Open Archaeology*, *2014*, 29–53.

Schneider, R., & Dyer, S. (2006). *Death by a thousand cuts: Impacts of in situ oil sands development on Alberta's boreal forest*. Edmonton, AB: Canadian Parks and Wilderness Society and the Pembina Institute.

Scott, A. (1994). *Oil exploitation and ecological problems in Siberia*. IIASA, Laxenburg, Austria: WP-94-023.

Shannon, R. D., & White, J. R. (1994). A three-year study of controls on methane emissions from two Michigan peatlands. *Biogeochemistry*, *27*, 35–60.

Strack, M., Waller, M. F., & Waddington, J. M. (2006). Sedge succession and peatland methane dynamics: A potential feedback to climate change. *Ecosystems*, *9*(2), 278–287. https://doi.org/10.1007/s10021-005-0070-1

Strack, M., Cagampan, J., Fard, G. H., Keith, A. M., Nugent, K., Rankin, T., et al. (2016). Controls on plot-scale growing season CO_2 and CH_4 fluxes in restored peatlands: Do they differ from unrestored and natural sites? UWSpace. Retrieved from http://hdl.handle.net/10012/11531

Strack, M., Softa, D., Bird, M., & Xu, B. (2017). Impact of winter roads on boreal peatland carbon exchange. *Global Change Biology*, *24*(1), e201–e212. https://doi.org/10.1111/gcb.13844

Sundh, I., Nilsson, M., Granberg, G., & Svensson, B. H. (1994). Depth distribution fo microbial production and oxidation of methane in northern boreal peatlands. *Microbial Ecology*, *27*(3), 253–265. https://doi.org/10.1007/BF00182409

Tuittila, E., Komulainen, V., & Vasander, H. (2000). Methane dynamics of a restored cut-away peatland. *Global Change Biology*, *6*(5), 569–581. https://doi.org/10.1046/j.1365-2486.2000.00341.x

van Rensen, C. K., Nielsen, S. E., White, B., Vinge, T., & Lieffers, V. J. (2015). Natural regeneration of forest vegetation on legacy seismic lines in boreal habitats in Alberta's oil sands region. *Biological Conservation*, *184*, 127–135. https://doi.org/10.1016/j.biocon.2015.01.020

van Winden, J. F., Reichard, G.-J., McNamara, N. P., Benthien, A., & Damsté, J. S. S. (2012). Temperature-induced increase in methane release from peat bogs: A mesocosm experiment. *PLoS One*, *7*(6), e39614. https://doi.org/10.1371/journal.pone.0039614

Vazquez-Amábile, G. G., & Engel, B. A. (2005). Use of SWAT to compute groundwater table depth and streamflow in the Muscatatuck River Watershed. *Transactions of ASAE*, *48*(3), 991–1003. https://doi.org/10.13031/2013.18511

Vitt, D. H., & Bhatti, J. S. (2012). *Restoration and reclamation of boreal ecosystems : Attaining sustainable development*. Cambridge: Cambridge University Press. https://doi.org/10.1017/CBO9781139059152

Wieder, R. K., & Vitt, D. H. (2006). *Boreal peatland ecosystems*. Berlin: Springer. https://doi.org/10.1007/978-3-540-31913-9

Williams, T. J., Quinton, W. L., & Baltzer, J. L. (2013). Linear disturbances on discontinuous permafrost: Implications for thaw-induced changes to land cover and drainage patterns. *Environmental Research Letters*, *8*(2). https://doi.org/10.1008/1748-9326/8/2/025006

Xu, K., Kong, C., Liu, J., & Wu, Y. (2010). Using methane dynamic model to estimate methane emission from natural wetlands in China. In *18th International Conference on Geoinformatics*. Beijing, Hebei: IEEE.

Zhu, Q., Liu, J., Peng, C., Chen, H., Fang, X., Jiang, H., et al. (2014). Modelling methane emissions from natural wetlands by development and application of the TRIPLEX-GHG model. *Geoscientific Model Development*, *7*, 981–999.